Anomalous Peak Intensities in the EXAFS of Polynuclear Molybdenum Compounds

Takafumi MIYANAGA, Takashi FUJIKAWA,† Nobuyuki MATSUBAYASHI,†† Takao FUKUMOTO, Kunihiko YOKOI,††† Iwao WATANABE,* and Shigero IKEDA††††

Department of Chemistry, Faculty of Science, Osaka University, Toyonaka, Osaka 560
†Faculty of Engineering, Yokohama National University, Yokohama 240
††National Chemical Laboratory for Industry, Yatabe, Ibaraki 305
†††Department of Chemistry, Osaka Kyoiku University, Ikeda, Osaka 563
††††Institute of Science and Technology, Ryukoku University, Fushimi-ku, Kyoto 612

(Received June 17, 1988)

EXAFS (Extended X-ray Absorption Fine Structure) experiments on various polynuclear molybdate and tungstate compounds revealed the unusual phenomenon that Mo-O peaks which should appear at around 1.9 Å in Fourier transforms of the EXAFS spectra for $Mo_6O_{19}^{2-}$ and $PMo_{12}O_{40}^{3-}$ are hardly discernible, while the tungstates and other molybdates give the metal-oxygen peaks normally. It is concluded that the Debye-Waller factors for the metal-bridging oxygen bonds in $Mo_6O_{19}^{2-}$ and $PMo_{12}O_{40}^{3-}$ are exceptionally large (≧ 0.08 Å). The shape of the Raman bands for the $Mo_6O_{19}^{2-}$ pertaining to the vibration involving the bridging oxygens supports the large σ values estimated. EXAFS measurements were also performed for $AsMo_{12}O_{40}^{3-}$, $SiMo_{12}O_{40}^{4-}$, and $PMo_{12}O_{40}^{3-}$. The compounds with large Debye-Waller factors seem to be unstable against reductants.

EXAFS studies of molybdenum compounds have been attempted because of their interesting structures[1,2] and their reactivity as catalysts.[3]

The hexavalent molybdenum ion exists as a monomeric form of MoO_4^{2-} in a neutral or alkaline solution. In an acidic solution, the ion exists in the form of either $Mo_7O_{24}^{6-}$, $Mo_8O_{26}^{4-}$, or $Mo_6O_{19}^{2-}$, depending on the acidity of the solution. Heteropoly complexes of the Keggin structure, e.g., $PMo_{12}O_{40}^{3-}$, also exist in the presence of the PO_4^{3-} ion. Other heteropoly complexes are also known in which the P atom is replaced with Si, As, or Ge. Some of the Mo(VI) atoms in the polynuclear complexes can be reduced to form so-called molybdenum-blue. The polytungstates, e.g., $W_6O_{19}^{2-}$ and $PW_{12}O_{40}^{3-}$, with structures similar to those of the corresponding molybdenum complexes, are also known.

These molybdates and tungstates have been isolated as crystals, and their structures have been determined by the X-ray diffraction method. According to the literature, molybdenum in MoO_4^{2-} is coordinated by four oxygen atoms with the Mo-O distances of 1.75—1.78 Å.[4] $Mo_7O_{24}^{6-}$ and $Mo_6O_{19}^{2-}$ are composed of seven and six MoO_6 distorted octahedral units, respectively. In $Mo_6O_{19}^{2-}$ (Fig. 1a), the Mo-O bond distances have been reported to be 1.68 Å for terminal double bonds, 1.86—2.01 Å for bridging oxygens, and 2.32 Å for a central bridging oxygen.[5] The heteropoly compound, $PMo_{12}O_{40}^{3-}$ (Fig. 1b), has similar octahedral units around a central phosphorous atom.[6] Although the interatomic distances in the compounds of tungstates are not exactly the same as those in molybdates, the geometrical structures of the molybdenum and tungsten polynuclear compounds are quite similar to each other, e.g., $Mo_6O_{19}^{2-}$/$W_6O_{19}^{2-}$, and $PMo_{12}O_{40}^{3-}$/$PW_{12}O_{40}^{3-}$.

During the course of the EXAFS studies of these

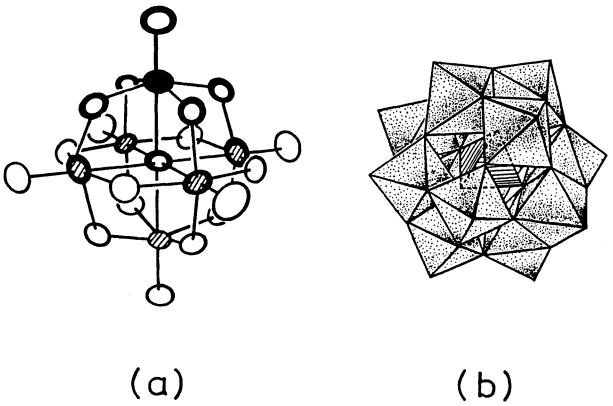

Fig. 1. (a) The structure of $Mo_6O_{19}^{2-}$ complex. The atoms circled with heavy line are included in the multiple scattering calculations. ◍ Molybdenum, ○ oxygen, and ● X-ray absorbing molybdenum atom. (b) The structure of Keggin type complex. Each octahedron represents MO_6 unit.

complexes in solution, we found the unusual phenomenon that the Mo-O peaks are hardly discernible in Fourier transforms for $Mo_6O_{19}^{2-}$ and $PMo_{12}O_{40}^{3-}$, while other molybdenum and tungsten compounds give normal peak intensities.[7] It is extremely important to know why the first shell atoms, which are normally the most easily detectable atoms by the EXAFS method, give almost no EXAFS peaks. Our lack of knowledge of the cause makes the use of the EXAFS technique too dangerous for structure analysis.

Since the anomalous peak intensities appear only for the samples of highly symmetrical $Mo_6O_{19}^{2-}$ and $PMo_{12}O_{40}^{3-}$, and not for low-symmetry samples (e.g., $Mo_7O_{24}^{6-}$), it is possible that this phenomenon is connected only to specified geometrical configurations. We must introduce a multiple-scattering the-

ory for the EXAFS analysis in order to discriminate between geometrical configurations, because the single-scattering theory treats only interatomic distances from the X-ray absorbing atom, i.e., the Mo-O and Mo-Mo distances. As far as Mo-O bonds are concerned, the single-scattering theory regards these complex polymers as simple MoO_6 octahedra. There is no room in the theory for the consideration of the symmetries of the complexes as to how the octahedral units are connected.

In the present paper, the origin for those anomalous peak intensities will be discussed from the points of view of the multiple-scattering effect and the Debye-Waller factor, which, of course, is a key parameter determining the peak intensities. Consequently, the large Debye-Waller factor for several molybdenum complexes are inferred and confirmed by the Raman spectroscopy.

Experimental

The $Na_2MoO_4 \cdot 2H_2O$, $(NH_4)_6Mo_7O_{24} \cdot 4H_2O$, and $Na_2WO_4 \cdot 2H_2O$ were purchased from Wako Pure Chemical Industries, Ltd., and the MoO_3, from the Merck Company. The $[(C_4H_9)_4N]_2Mo_6O_{19}$,[8] $[(C_4H_9)_4N]_2W_6O_{19}$,[9] $PMo_{12}O_{40}^{3-}$-TBA ($(C_4H_9)_4N^+$) salt, $AsMo_{12}O_{40}^{3-}$-TBA salt, $SiMo_{12}O_{40}^{4-}$-TBA salt, and $PW_{12}O_{40}^{3-}$-TEA($(C_2H_5)_4N^+$) salt were prepared according to the literature.[10] A partially reduced species of $PMo_{12}O_{40}^{3-}$, molybdenum-blue, was prepared by the reduction with ascorbic acid. The X-ray absorption spectra of Mo K-edge and W L_{III}-edge were obtained at BL-7C and 10B of the Photon Factory of the National Laboratory for High Energy Physics (KEK). The storage ring was operated at 2.5 GeV, and the ring current was between 150—200 mA. A Si(111) double-crystal monochromator and a Si(311) channel-cut crystal monochromator were used. The solid samples were powdered and loaded on adhesive tapes. The liquid samples were placed in a polyethylene pouch.

The Raman spectra of the powdered samples were measured with an Ar ion laser (5145 Å) at room temperature and at 88 K.

Data Analysis and Calculations

The EXAFS data treatments have been described in detail elsewhere,[11] and so they will be only briefly treated in this section. The EXAFS oscillation $\chi(k)$ is extracted from the absorption spectrum $\mu(k)$ as follows:

$$\chi(k)=[\mu(k)-\mu_0(k)]/\mu_0(k). \quad (1)$$

The background absorption $\mu_0(k)$ is obtained from the least-square fitting of the pre-edge region (about 300 eV) to the Victoreen formula, $a\lambda^3-b\lambda^4+c$, where a, b, and c are the constants and where λ is the wavelength of the incident X-ray. The c constant is introduced in order to correct the difference in the sensitivities of the ionization detectors for I and I_0. In order to remove low-frequency noises from $\chi(k)$, the following method is used. The second-order seven-point smoothing is applied to the $\chi(k)$ data until only the lowest-frequency component of significant signals remains. Subsequently, a base line is obtained by using a third-order natural spline method with which the center points of the oscillation in the smoothed spectrum are connected. Thus, the low-frequency noises are removed from $\chi(k)$ by subtracting the base line obtained. In the single-scattering approximation, the extracted EXAFS is described as:

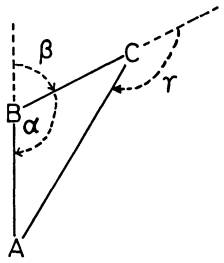

Fig. 2. Schematic representation of a triatomic system. A is the X-ray absorbing atom, and B and C are the scattering atoms.

$$\chi(k)=\sum_j S_j k^{-1} N_j r_j^{-2} f_j(k) \exp(-2r_j/\eta) \exp(-2k^2\sigma_j^2) \times \sin[2kr_j+\psi_j(k)], \quad (2)$$

where k is the photoelectron wave vector defined as:

$$k=[2m(E-E_0)]^{1/2}/\hbar. \quad (3)$$

E and E_0 are the photon energy and the threshold energy, respectively. S_j is the damping factor by the multielectron effect, m is the mass of an electron, N_j is the number of atoms located at distance r_j, η is the mean free path of the photoelectron, and σ_j is the root-mean-square displacement of r_j (the RMSRD or Debye-Waller factor). The backscattering amplitude $f_j(k)$ and the phase shift $\psi(k)$ calculated by Teo and Lee[12] are used for the Fourier transforms. The energy at the half height of the edge jump is used as the value of E_0.

The multiple-scattering calculations for EXAFS are performed according to the following equation for the triatomic model (A,B,C) shown in Fig. 2:[13,14]

$$\begin{aligned}\chi_{AC}(k)=&[(-1)^l/k]\{f_C(\pi)\exp(-2\sigma_{AC}^2k^2)\\ &\times\sin[2kr_{AC}+2\delta_l+\psi_C(\pi)]/r_{AC}^2+[2\cos(\gamma-\alpha)f_B(\beta)f_C(\gamma)/\\ &(r_{AB}r_{BC}r_{AC})]\exp[-(1-\cos\beta)^2k^2\sigma_{AB}^2/2]\\ &\times\exp[-(1-\cos\gamma)^2k^2\sigma_{AC}^2/\\ &2]\sin[k(r_{AB}+r_{BC}+r_{AC})+2\delta_l+\psi_B(\beta)\psi_C(\gamma)]+[f_B(\beta)^2f_C(\pi)/\\ &(r_{AB}^2r_{BC}^2)]\exp[-(1-\cos\beta)^2k^2\sigma_{AB}^2]\exp(-2k^2\sigma_{BC}^2)\\ &\times\sin[2k(r_{AB}+r_{BC})+2\delta_l+2\psi_B(\beta)+\psi_C(\pi)]\},\end{aligned} \quad (4)$$

where δ_l is the phase shift of the central atom with an angular momentum l and where ψ is that of the scattering atom. The muffin-tin potential of atoms with a neutral charge is assumed for the scattering field.

Results

EXAFS Spectra. Figure 3 shows the Fourier transforms of the Mo K-edge EXAFS for molybdenum com-

pounds and of the W L_{III}-edge EXAFS for tungsten compounds. The peak corresponding to Mo-O is present at 1.77 Å in the spectrum for MoO_4^{2-} (Fig. 3a). In the spectrum for MoO_3 (Fig. 3b), two peaks corresponding to Mo-O and Mo-Mo appear at 1.79 Å and 3.60 Å, respectively. Although several Mo-O bonds with different lengths are present in $Mo_7O_{24}^{6-}$, the bonds give only a single peak at 1.75 Å in the Fourier transform, and the Mo-Mo peak lies at 3.20 Å in the spectrum (Fig. 3c).

To our great surprise, we find quite an unusual phenomenon in the Fourier transform spectrum for $Mo_6O_{19}^{2-}$ (Fig. 3d). That is, the Mo-O peaks for the complex which should appear at somewhere around 1.9 Å are hardly discernible, while a high and sharp peak corresponding to the oxygen-bridged Mo-Mo distance appears at 3.26 Å. The X-ray diffraction results predict that both the Mo-O and Mo-Mo peaks for $Mo_6O_{19}^{2-}$ should be higher than those for $Mo_7O_{24}^{6-}$, since the structure of $Mo_6O_{19}^{2-}$ is highly symmetrical compared to $Mo_7O_{24}^{6-}$.[15] The EXAFS measurements were repeated at 20 K in order to study the effect of thermal vibration on the peak height for the Mo-O bonds. The result, shown as a broken line in Fig. 3d, is essentially the same as that obtained at room temperature. This indicates that the disappearance of the peak is not caused by the thermal vibration. In contrast to the result for $Mo_6O_{19}^{2-}$, the spectrum for $W_6O_{19}^{2-}$ is quite normal (Fig. 3f); there are two peaks corresponding to the terminal W=O (1.66 Å) and the bridging W-O (1.96 Å) bonds in addition to a W-W peak (3.45 Å).

An analogous phenomenon appears in heteropoly acids, as is shown in Fig. 4. The Mo-O peaks are very much obscured in the spectrum for $PMo_{12}O_{40}^{3-}$ (a), while peaks corresponding to W=O (1.60 Å) and W-O (1.98 Å) appear in that for $PW_{12}O_{40}^{3-}$(b). However, the Mo-O peak appears at 1.92 Å in the spectrum for the reduced $PMo_{12}O_{40}$ species (c).

$AsMo_{12}O_{40}^{3-}$ and $SiMo_{12}O_{40}^{4-}$ form the same structure as $PMo_{12}O_{40}^{3-}$. In the spectrum for $AsMo_{12}O_{40}^{3-}$ (d), the Mo-O peaks are poorly characterized, in a manner similar to that found for $PMo_{12}O_{40}^{3-}$ (a), whereas the Mo-O peak appears rather clearly at 1.85 Å in the spectrum for $SiMo_{12}O_{40}^{4-}$ (e).

Multiple-Scattering Calculation. The EXAFS analysis are normally done using a single-scattering theory. In this section we will study whether a photoelectron standing wave can be diminished for the system taking a special geometrical arrangement of scattering atoms due to a multiple-scattering effect, thus causing the peak in the Fourier transform to disappear. Figure 5 shows the calculated EXAFS oscillation spectra and their Fourier transforms, which were obtained by the use of the single-scattering (solid line) and multiple-scattering (broken line) theories. The atoms marked with a heavy line in Fig.

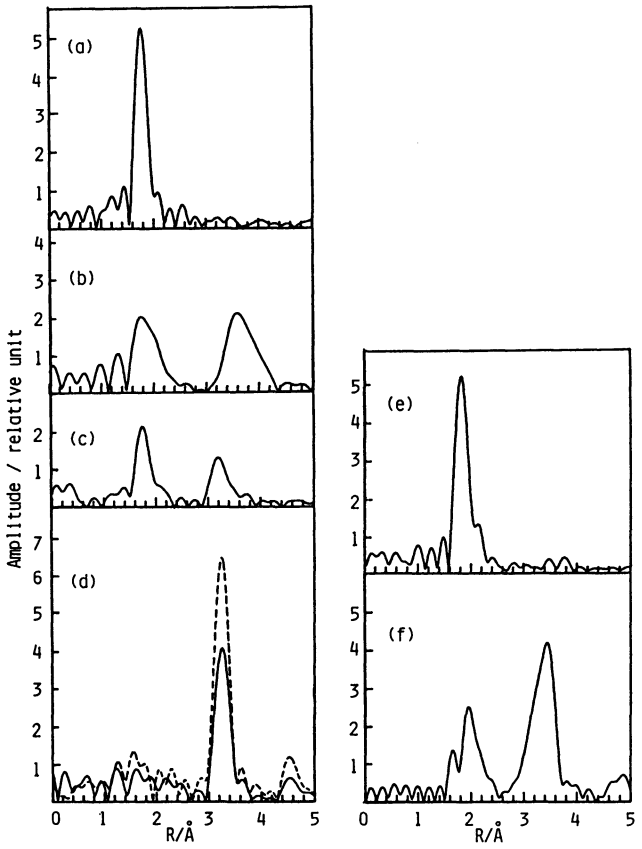

Fig. 3. Fourier transforms of Mo K-edge EXAFS for (a) $Na_2MoO_4 \cdot 2H_2O$, (b) MoO_3, (c) $(NH_4)_6Mo_7O_{24} \cdot 4H_2O$, (d) $[(C_4H_9)_4N]_2Mo_6O_{19}$, and WL$_{III}$-edge EXAFS for (e) $Na_2WO_2 \cdot 2H_2O$, and (f) $[(C_4H_9)_4N]_2W_6O_{19}$. Broken line in (d) represents that measured at 20 K.

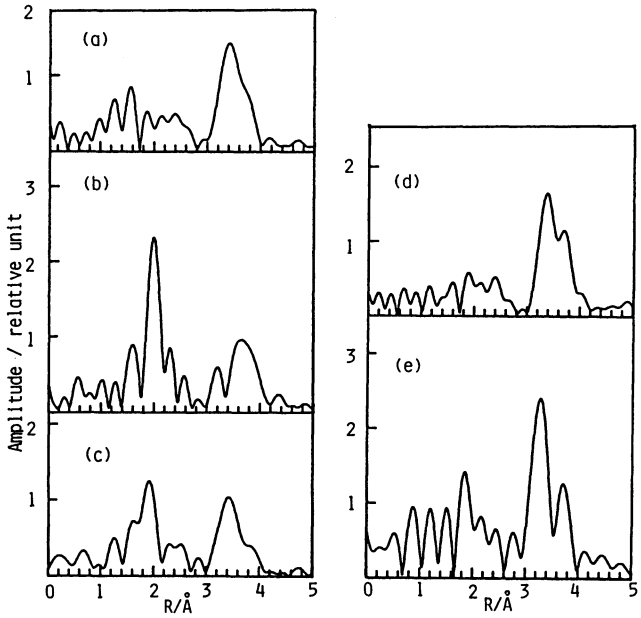

Fig. 4. Fourier transforms of Mo K-edge and W L_{III}-edge EXAFS for (a) $PMo_{12}O_{40}^{3-}$, (b) $PW_{12}O_{40}^{3-}$, (c) the reduction product from $PMo_{12}O_{40}^{3-}$, (d) $AsMo_{12}O_{40}^{3-}$ and (e) $SiMo_{12}O_{40}^{4-}$.

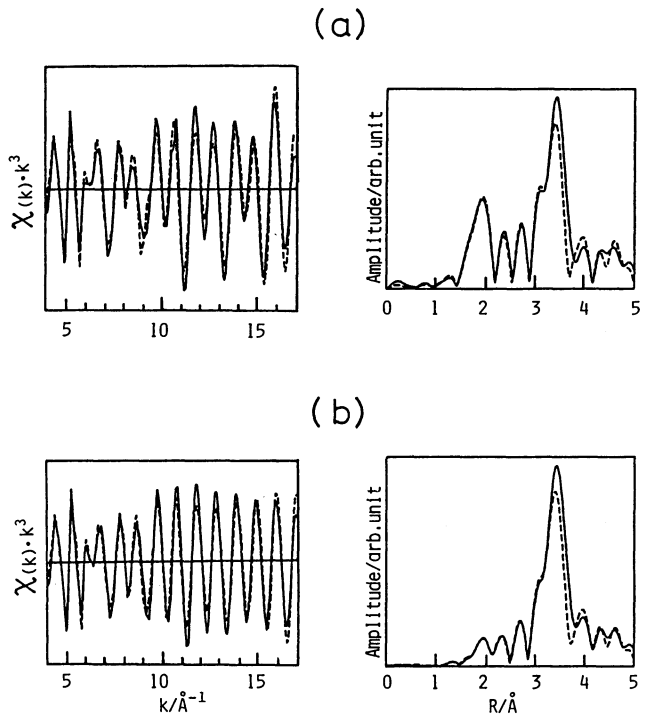

Fig. 5. Calculated EXAFS spectra and their Fourier transforms for the model compound for $Mo_6O_{19}^{2-}$. The σ values used for Mo-O are (a) 0.04 Å and (b) 0.08 Å. Solid line and broken line represent the result of the single scattering and multiple scattering calculations, respectively.

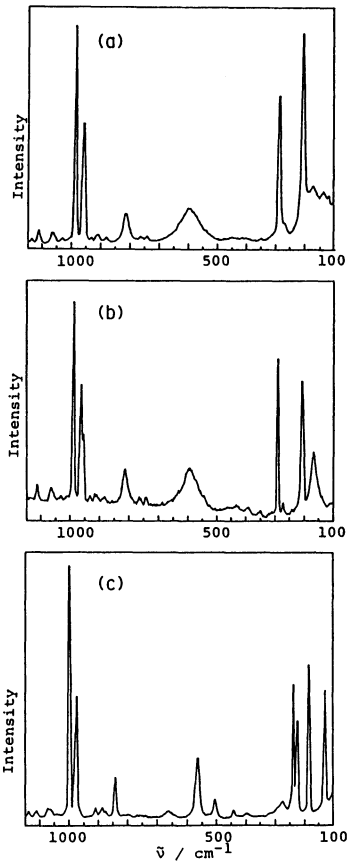

Fig. 6. Raman spectra for (a) $[(C_4H_9)_4N]_2Mo_6O_{19}$ at room temperature, (b) at 88 K, and (c) $[(C_4H_9)_4N]_2W_6O_{19}$ at room temperature.

1a constitute the MoO_6Mo_4 cluster used for the calculations of the model of $Mo_6O_{19}^{2-}$. The positions of the atoms are given from the crystallographic data.[5] Figure 5a shows the results obtained using the Debye-Waller factor σ of 0.04 Å for both Mo-O and Mo-Mo bonds. The value of 0.04 Å has been determined by Cramer et al.[1] in the case of the Mo(V) dimer. No significant difference can be observed between the single-scattering and multiple-scattering results. The calculations predict the Mo-O peaks at 1.7—2.0 Å and the Mo-Mo peak at 3.3 Å, as normal. Since the peak intensity depends upon the Debye-Waller factor, the simulation calculations were also performed using different σ values. Figure 5b shows the results for the case in which the σ value of 0.08 Å for the Mo-O bond is used. The value of 0.08 Å was selected according to the results of a Raman study, which will be discussed in the Discussion section below. The Mo-O peak at about 2.0 Å can no longer be distinguished from the ripple peaks.

Raman Spectra. A noteworthy difference in the Raman spectra is observed in the shape of the peak corresponding to the vibration involving the metal-bridging oxygen bond between the samples of $Mo_6O_{19}^{2-}$ and $W_6O_{19}^{2-}$. The Raman spectrum for $Mo_6O_{19}^{2-}$ at room temperature has a very broad peak at ca. 600 cm^{-1}, as is shown in Fig. 6a. Cooling the sample down to 88 K causes only a small reduction in the width of the peak, as is shown in Fig. 6b. According to the literature,[16] the peaks at ca. 600 cm^{-1} for $Mo_6O_{19}^{2-}$ and 570 cm^{-1} in Fig. 6c for $W_6O_{19}^{2-}$ have been assigned to correspond to the symmetrical stretching vibration of the bridging M-O-M bond (M=metal). It is remarkable that this peak for $Mo_6O_{19}^{2-}$ is significantly broader than that for $W_6O_{19}^{2-}$, while the peaks at ca. 1000 cm^{-1} due to the terminal M=O bonds are quite similar to each other. The peak at 167 cm^{-1} which has been assigned to the Mo-O-Mo bending vibration in the $Mo-O_4$ plane is also broad, and its width changes with the temperature.

Discussion

Our results definitely show that the anomalously low peak intensity for $Mo_6O_{19}^{2-}$ arises from the large Debye-Waller factor of the Mo-O bond in this compound. The theoretical calculations do not predict that the multiple-scattering effect works on the very specified symmetrical geometry of $Mo_6O_{19}^{2-}$ complex to diminish certain peaks. The calculations predict, instead, that the disappearance of the peaks can easily occur with larger σ values. The large σ value of the bond seems to be related to the anomalous peak shapes

in its Raman spectrum.

The σ value in the theory of EXAFS is given by:

$$\sigma^2 = \sigma^2_{stat} + \sigma^2_{vib.} \quad (5)$$

Thus, it is divided into static and vibronic contributions. The static factor represents the distribution of interatomic distances. As is obvious from the low symmetry of $Mo_7O_{24}^{6-}$, it is known from the X-ray diffraction study that the complex has Mo-O_{bridge} bonds with various lengths in it.[15] The bond lengths of Mo-O spread from 1.8 to 2.5 Å in $Mo_7O_{24}^{6-}$, while those in $Mo_6O_{19}^{2-}$ spread from 1.86 to 2.01 Å.[17] Therefore, the static factor must be much larger for $Mo_7O_{24}^{6-}$ than for $Mo_6O_{19}^{2-}$. Consequently, the present EXAFS results indicate that the apparent large σ value for $Mo_6O_{19}^{2-}$ comes not from the static part, but from the vibronic one. As for $W_6O_{19}^{2-}$, there are two reports which are inconsistent with each other with respect to the W-O bond lengths.[18,19]

Recently, the relationship between the Raman spectrum and the EXAFS Debye-Waller factor was studied by Lottici.[20] From his study of the nearest neighbor central force (NNCF) model, which is more exact than the Einstein model, he reported that the Debye-Waller factor can be related to the relative (or projected) density of vibrational states ρ_R. According to the Einstein model, the calculated σ_{vib} values of the M-O bond for $Mo_6O_{19}^{2-}$ and $W_6O_{19}^{2-}$ must be nearly equal because the vibrational frequencies for the M-O bonds in the two compounds are nearly equal. Thus, this model is not adequate for an attempt to find the cause of the difference in the character of the M-O bonds. The value of σ_{vib} is expressed[20] in terms of $\rho_R(\omega)$ according to the NNCF model as follows:

$$\sigma^2_{vib} = (\hbar/2\mu)\int[\rho_R(\omega)/\omega]\coth(\hbar\omega/2k_BT)d\omega. \quad (6)$$

The $\rho_R(\omega)$ is approximately related to the Raman scattering intensity $I(\omega)$ as follows:

$$I(\omega) = C\,\rho_R(\omega), \quad (7)$$

where C is the normalization constant. Now, using the above two relations, we can calculate the ratio of the σ_{vib} value of $Mo_6O_{19}^{2-}$ against that of $W_6O_{19}^{2-}$ with respect to the metal-bridging oxygen bonds from the Raman peaks of symmetrical stretching vibration at ca. 600 cm^{-1} and 570 cm^{-1}, respectively. The Raman intensities of the corresponding peaks are normalized by using one of the peaks due to the tetrabutylammonium ion at ca. 1060 cm^{-1}. The result of the calculation for the bridging oxygen gives a value of about 2 for the $\sigma_{vib}[Mo]/\sigma_{vib}[W]$ ratio. Therefore, once the σ_{vib} value of 0.04 Å for the W-O bond in $W_6O_{19}^{2-}$, which is a very typical value for metal complexes, is adopted for the EXAFS simulation calculation, the σ_{vib} value of 0.08 Å must be employed for the calculation of $Mo_6O_{19}^{2-}$. The EXAFS simulation calculations using these σ values show that the σ value of 0.04 Å is small enough to present the M-O peak in the Fourier transform, while the value of 0.08 Å is too large to present the peak, as is indicated in Fig. 5.

The EXAFS spectrum taken at 20 K for $Mo_6O_{19}^{2-}$ (Fig. 3d) indicates that the apparent σ value does not depend on the temperature. The same is true for the σ_{vib} value estimated from the Raman spectra taken at room temperature (Fig. 6a) and at 88 K (Fig. 6b). Equation 6 shows that, even at $T=0$, σ_{vib} has a finite value proportional to $\rho_R(\omega)/\omega$. The present study concludes that the Mo-O bond in $Mo_6O_{19}^{2-}$ has a large σ_{vib} value in which the temperature-independent contribution dominates. (As a matter of fact, for the vibration of $\omega=600$ cm^{-1}, the value of $\coth(\hbar\omega/2k_BT)$ is almost 1 throughout all the range from $T=0$ to room temperature.)

We speculate that the large σ value for Mo-O bond is related to the rotational vibration on the axis of $O_{terminal}$-Mo-O_{center} (the rotation of the plane including four O_{bridge}'s); thus, the vibrational peaks corresponding to the Mo-O_{bridge} stretching vibration (at ca. 600 cm^{-1}) and the O_{bridge}-Mo-O_{bridge} bending (at ca. 160 cm^{-1}) are broad in the Raman spectrum because of the coupling of these vibrations to the rotational vibration. This interpretation is compatible with the EXAFS result of the clear appearance of the distant bond, Mo-Mo, in $Mo_6O_{19}^{2-}$ inspite of the disappearance of the shorter bond Mo-O_{bridge}, because the rotation does not change the Mo-Mo, but the Mo-O distance.

In concluding this section, it should be mentioned that there is something puzzling in the results of the X-ray diffraction analyses (XDA) of the complexes. None of the reported values of thermal parameters in XDA for Mo and W complexes contain any indication which can be connected to either the large σ values inferred from the EXAFS analyses or the broad band shapes in the Raman spectra. In either case in which static or vibronic disorder causes the peak disappearance in EXAFS of $Mo_6O_{19}^{2-}$, the values of the thermal parameters in XDA for O_{bridge} in it can be expected to be large. The incompatibility between the results of EXAFS and XDA requires further study in this regard.

Reactivity as Oxidants. It is interesting to note that $Mo_6O_{19}^{2-}$, $PMo_{12}O_{40}^{3-}$, and $AsMo_{12}O_{40}^{3-}$, for which the Mo-O peaks disappear in the Fourier transforms, are the most easily reducible species among the molybdenum complexes. According to the empirical classification by Pope,[21] the reactivity of $Mo_6O_{19}^{2-}$ as the oxidant is higher than that of $Mo_7O_{24}^{6-}$. Judging from the electrochemical redox potentials, the orders of reactivities are $PMo_{12}O_{40}^{3-} > PW_{12}O_{40}^{3-}$,[22] and $AsMo_{12}O_{40}^{3-} > PMo_{12}O_{40}^{3-} > SiMo_{12}O_{40}^{4-}$.[23] This is perfectly in accordance with the fact that $Mo_7O_{24}^{6-}$, $PW_{12}O_{40}^{3-}$, and $SiMo_{12}O_{40}^{4-}$ show the Mo-O peaks in their Fourier transforms. Thus, the compounds with high redox potentials are electrically unstable, even though they take highly symmetrical structures. It has also been reported that the redox reaction of

$PMo_{12}O_{40}^{3-}$ with hydrogen and isotopically labeled oxygen exchanges bridging oxygen atoms far more easily than the terminal oxygens.[24] Further, the Raman[24] and IR[25] spectroscopic studies and the Xα MO calculation[26] have indicated that the bridging oxygen atoms are more reactive than the terminal oxygens. From the point of view of reactivity as the oxidant, the intensity of the M-O peak in the Fourier transform seems to be small for a species with highly reactive bridging oxygen atoms. From the evidence in the present study, the M-O bonds in highly reactive molybdenum complexes can be considered to be "strained bonds" which may be created by the stress of the large framework of the polynuclear compounds. It has been reported that there is a correlation between the Debye-Waller factors determined from EXAFS experiments on aqua metal complexes and their ligand-water exchange-reaction rates.[27] The present study provides another example of the correlation between the Debye-Waller factor and the chemical reactivity.

Conclusion

Some of the molybdenum polynuclear compounds show almost no peaks corresponding to metal-oxygen bonds in their Fourier transforms of the EXAFS spectra. This very strange fact is the result of the large Debye-Waller factor of the corresponding bonds. This conclusion is supported by the theoretical simulation calculations and the results of the Raman spectroscopy. The metal-bridging oxygen bonds in those compounds must be deformed to make these compounds reactive toward a redox reaction.

The present authors wish to thank Drs. Tadashi Matsushita and Masaharu Nomura of the National Laboratory for High Energy Physics (KEK) for their help with the X-ray absorption measurements. This work was supported by a Grant-in-Aid for Special Project Research (No.62124039) from the Ministry of Education, Science and Culture.

References

1) S. P. Cramer, P. K. Eiden, M. T. Paffett, J. R. Winkler, Z. Dori, and H. B. Gray, *J. Am. Chem. Soc.*, **105**, 799 (1983).
2) K. Yokoi, N. Matsubayashi, T. Miyanaga, I. Watanabe, K. Murata, and S. Ikeda, *Chem. Lett.*, **1987**, 1453.
3) Y. Iwasawa, K. Asakura, H. Ishii, and H. Kuroda, *Z. Phys. Chem. Neue Folge*, **144**, 105 (1985).
4) K. Matsumoto, A. Kobayashi, and Y. Sasaki, *Bull. Chem. Soc. Jpn.*, **48**, 1009 (1975).
5) O. Nagano and Y. Sasaki, *Acta Crystallogr., Sect. B*, **35**, 2387 (1979).
6) R. Strandberg, *Acta Chem. Scand., Ser. A*, **29**, 359 (1975).
7) T. Miyanaga, N. Matsubayashi, T. Fukumoto, K. Yokoi, I. Watanabe, K. Murata, and S. Ikeda, *Chem. Lett.* **1988**, 487.
8) K. Murata, E. Yamamoto, and S. Ikeda, *Bull. Chem. Soc. Jpn.*, **56**, 941 (1983).
9) M. Boyer and B. L. Meur, *C. R. Acad. Sci. Paris*, **1975**, 281.
10) A. Rosenheim and J. Jaenicke, *Z. Anorg. Allog. Chem.*, **101**, 248 (1917).
11) N. Matsubayashi, Thesis, Osaka University (1986).
12) B. K. Teo and P. A. Lee, *J. Am. Chem. Soc.*, **101**, 2815 (1979).
13) B. K. Teo, *J. Am. Chem. Soc.*, **103**, 3990 (1981).
14) T. Fujikawa, *J. Phys. Soc. Jpn.*, **54**, 2747 (1985).
15) H. T. Evans, B. M. Gatehouse, and P. Leverett, *J. Chem. Soc., Dalton Trans.*, **1975**, 505
16) R. Mattes, H. Bierbusse, and J. Fuchs, *Z. Anorg. Allg. Chem.*, **385**, 230 (1971).
17) H. R. Allcock, E. C. Bissell, and E. T. Shawl, *Inorg. Chem.*, **12**, 2963 (1973).
18) G. Henning and A. Hüllen, *Z. Kristallogr.*, **30**, 162 (1969).
19) J. Fuchs, W. Freiwald, and H. Hartl, *Acta Crystallogr., Sect. B*, **34**, 1764 (1978).
20) P. P. Lottici, *Phys. Rev. B*, **35**, 1236 (1987).
21) M. T. Pope, *Inorg. Chem.*, **11**, 1973 (1972).
22) M. Otake and T. Onoda, *Shokubai*, **18**, 169 (1976); K. Katamura, T. Nakamura, K. Sakata, M. Misono, and Y. Yoneda, *Chem. Lett.*, **1981**, 89.
23) K. Eguchi, T. Seiyama, N. Yamazoe, S. Katsuki, and H. Taketa, *J. Catal.*, **111**, 336 (1988).
24) H. Tsuneki, H. Niiyama, and E. Echigoya, *Chem. Lett.*, **1978**, 1183.
25) K. Eguchi, Y. Toyozawa, K. Furuta, N. Yamazoe, and T. Seiyama, *Chem. Lett.*, **1981**, 1253.
26) H. Taketa, S. Katsuki, K. Eguchi, T. Seiyama, and N. Yamazoe, *J. Phys. Chem.*, **90**, 2959 (1986).
27) T. Miyanaga, I. Watanabe, and S. Ikeda, *Chem. Lett.*, **1988**, 1073.